Molecular Crystals and Liquid Crystals Science and Technology. Section A. Molecular Crystals and Liquid Crystals

Publication details, including instructions for authors and subscription information:
http://www.tandfonline.com/loi/gmcl19

Dynamics of Microconfined Nematic Liquid Crystals and Related NMR Studies

S. Žumer [a], P. Ziherl [a] & M. Vilfan [b]

[a] Department of Physics, University of Ljubljana, Jadranska 19, 1111, Ljubljana, Slovenia

[b] J. Stefan Institute, University of Ljubljana, Jamova 39, 1111, Ljubljana, Slovenia

Version of record first published: 24 Sep 2006

To cite this article: S. Žumer, P. Ziherl & M. Vilfan (1997): Dynamics of Microconfined Nematic Liquid Crystals and Related NMR Studies, Molecular Crystals and Liquid Crystals Science and Technology. Section A. Molecular Crystals and Liquid Crystals, 292:1, 39-59

To link to this article: http://dx.doi.org/10.1080/10587259708031919

Mol. Cryst. Liq. Cryst., 1997, Vol. 292, pp. 39–59
Reprints available directly from the publisher
Photocopying permitted by license only

Dynamics of Microconfined Nematic Liquid Crystals and Related NMR Studies

S. ŽUMER[a,*], P. ZIHERL[a] and M. VILFAN[b]

[a]*Department of Physics, University of Ljubljana, Jadranska 19, 1111 Ljubljana, Slovenia;*
[b]*J. Stefan Institute, University of Ljubljana, Jamova 39, 1111 Ljubljana, Slovenia*

Different types of molecular motion in confined nematic liquid crystals are briefly discussed with emphasis on their detectability by methods of nuclear magnetic resonance and relaxation. The review is illustrated by some recent experimental and theoretical results in this field.

Keywords: Nematic liquid crystals; molecular dynamics; confined systems; nuclear magnetic relaxation and resonance; pulsed gradient spin-echo

PACS number(s): 64.70.Md, 76.90.+d

1. INTRODUCTION

Polymer dispersed liquid crystals (PDLC') [1], polymer stabilized cholesteric textures [2], and volume stabilized ferroelectric liquid crystals [3] are becoming increasingly important for electrooptic applications [4, 5]. In addition, these systems are fascinating by themselves. With a high surface-to-volume ratio, they provide unique possibility to study the effects of surface interactions and confining geometries on liquid crystalline ordering. This development stimulated also the research of liquid crystals confined to cavities of regular or irregular shape which are not directly related to applications but are rather well defined systems for investigations of these

*Corresponding author.
Phone: 386 61 265 061; Fax: 386 61 217 281; E-mail: Slobodan.zumer@fnt.uni-lj.si.

phenomena. Nuclepore and Anopore membranes [6, 7], Vycor glass [8] and various aerogels [9] were particularly useful: in these systems the internal surface of the pores can be treated chemically, which provides control of the liquid crystal-substrate interaction. Low polymer concentration materials — where polymer networks are dispersed in liquid crystals — have recently also attracted a lot of attention [10]. The common feature of all these systems is a competition of intrinsic ordering with surface and field induced effects yielding a large variety of peculiar and inhomogeneously ordered structures.

Both structure and dynamics of microconfined liquid crystals are predominantly influenced by the spatial constraints and surface coupling. Here we focus our attention to nematic phases: the molecular dynamics of these systems can be very effectively studied by nuclear magnetic resonance (NMR) methods which are sensitive to internal, orientational, and translational molecular motion and collective fluctuations associated with the characteristic order parameters. Molecular motion provides an averaging mechanism which in the NMR spectrum masks all details smaller than the characteristic rate of motion expressed in frequency units [11]. Therefore, the shape of the spectrum can yield only limited information concerning molecular dynamics. More detailed understanding of the underlying processes can be obtained by nuclear magnetic relaxation measurements, which can be used to study the molecular dynamics in liquid crystals on a broad time scale from 10^{-11} s to 10^{-5} s [12–14] and also in the ms range [15]. In addition, spin-echo experiments offer a direct insight into molecular diffusion [16].

Section 2 of this review covers dynamics in bulk systems and its relation to NMR. In Section 3 the main characteristics of the microconfined systems are discussed. Section 4 is concerned with the line shape and motional averaging and Section 5 is devoted to specific dynamics in such systems and its effects on the nuclear magnetic relaxation. A recent theoretical analysis of a nuclear spin-echo study of molecular diffusion in cylindrical cavities is presented in Section 6. Section 7 concludes the review.

2. DYNAMICS OF BULK NEMATIC PHASES AND NMR METHODS

Generally, the nematic liquid crystalline phase is described by a traceless tensorial order parameter $\underline{Q}$ [17], characterized by two eigenvalues (nematic order parameter and biaxiality) and three angles specifying the orientation of the eigenframe in space. In naturally uniaxial nematic phases — which are

most common — a weak biaxiality can be induced either by strong deformations or strong surface coupling. Since neither of these situations is essential for our discussion of dynamics, we restrict the treatment to uniaxial nematic ordering. This allows us to describe the ordering of the system by position-dependent nematic order parameter $S(\mathbf{r})$ and director $\mathbf{n}(\mathbf{r})$. The order parameter S is defined as the average $\langle 3\cos^2\theta_m - 1\rangle/2$, where θ_m is the angle between $\mathbf{n}$ and the molecular axis $\mathbf{m}$ (Fig. 1). In the bulk sample exposed to the constant magnetic field, the nematic director completely orients along the field. Even in such homogeneous bulk nematic liquid crystal the dynamics of molecules is rather complicated. It can be roughly divided into four main types:

Conformational changes — an internal motion which strongly depends on the molecular structure. The characteristic correlation times range between 10^{-10} and 10^{-12} s and do not change much when going from nematic to isotropic phase.

Individual molecular reorientation around the long axis and its fluctuations is in the upper MHz range. The frequencies of individual head-to-tail 180° reorientations around the short molecular axes are in the lower MHz range.

Translational self-diffusion in the liquid crystalline phase is an anisotropic molecular motion usually characterized by the diffusion tensor $\underline{D}$. For an unconstrained nematic phase $\underline{D}$ is uniaxial and the anisotropy is small, $D_\parallel/D_\perp \sim 2$ (where $\parallel$ stands for the direction parallel to the nematic director and $\perp$ for the direction perpendicular to it) [18]. Close to the nematic-

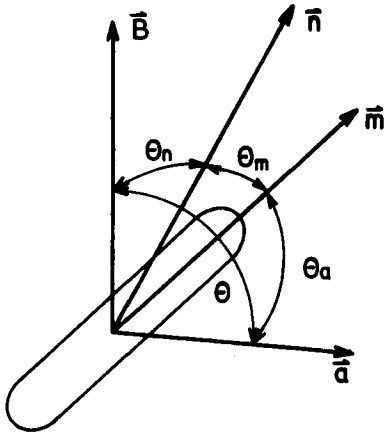

FIGURE 1 The angles, needed to describe the orientation of the internuclear vector **a** with respect to the direction of the magnetic field **B**, molecular axis **m**, and director **n**.

isotropic transition temperature, $D_\parallel$ is slightly above the value of the isotropic diffusion coefficient and $D_\perp$ is somewhat below it. If the symmetry of local molecular motions is broken by presence of a surface or a strong distortion, the nematic phase becomes biaxial [19] and the diffusion tensor is no longer uniaxial. Since all this effects are weak, the diffusion tensor is usually assumed to be the isotropic, the value of the diffusion coefficient D ranging between 10^{-10} ánd 10^{-12} m^2/s [18]. The average square of the molecular displacement in a time interval Δt is thus given by the well known relation $\langle(\Delta r)^2\rangle \approx 6D\Delta t$. By replacing $\sqrt{\langle(\Delta r)^2\rangle}$ with a typical intermolecular distance one can estimate the characteristic modulation time of the intermolecular coupling: it ranges between 10^{-7} and 10^{-9} s. On the other hand, just above the nematic-isotropic transition the nematic clusters appear in the isotropic phase. Such ordered regions are of the size of the correlation length $\xi = \xi_0\sqrt{T^*/(T-T^*)}$ where the supercooling limit T^* is usually about 1 K below the nematic-isotropic transition temperature and ξ_0 is comparable to the molecular size. As the molecule diffuses from the isotropic region into a cluster (or vice versa), the effective order parameter is modulated on the time scale 10^{-7}–10^{-8} s.

Order director fluctuations (ODF) —a collective orientational motion of molecules in the orientationally ordered phase—are characterized by a broad frequency distribution of thermally activated modes whose relaxation times are related to the elastic constant K and rotational viscosity γ_1 by the dispersion relation $\tau_2 \sim \gamma_1/Kq^2$, where q is the wave vector of the fluctuations [17]. Typical values of τ_2 range from 10^{-8} s for wave lengths comparable to the size of the molecules to 10^{-3} for micrometer wave lengths.

The first three types of motion occur in both isotropic and nematic phase but are anisotropic only in the latter case. ODF's, on the other hand, are characteristic for the nematic phase; in the isotropic phase, they are important only in pretansitional clusters with partial orientational order.

In order to relate the order parameter S to the observed line splitting in the **NMR spectrum** some questions about averaging over molecular motion must be answered. Let us examine a proton pair located on a liquid crystal molecule and characterized by an interproton vector **a**. In the isotropic phase the dipolar coupling is averaged out by isotropic molecular motion which results in a single NMR line with a natural width $\delta\nu < 100$ Hz. In the nematic phase the molecular dynamics becomes anisotropic and the non-averaged dipolar coupling yields a line splitting given by the well know relation

$$\Delta\nu = \Delta\nu_0|\langle 3\cos^2\theta - 1\rangle|/2 \qquad (1)$$

where $\Delta\nu_0$ is the strength of the dipolar coupling in frequency units [11] and θ is the angle between **a** and the magnetic field. The average is essentially performed over all motions with correlation times shorter than the characteristic time of the NMR experiment. Here this time is determined by $\Delta\nu^{-1}$, which, for a typical nematic, ranges between 10^{-5} and 10^{-4} s depending on the source of the splitting. The same relation [Eq. (1)] describes also the splitting caused by the quadrupolar coupling [11].

To examine the effect of the above motions, one has to introduce angles θ_a and θ_n in addition to θ_m and θ (Fig. 1). Here θ_a stands for the relative orientation of the vector **a** against molecular axis **m** and θ_n corresponds to the relative angle of director **n** against the external field, the deflection being caused by director fluctuations. In terms of these quantities,

$$\Delta\nu = \Delta\nu_0 S |\langle 3\cos^2\theta_a - 1\rangle_{\text{conf}} \langle 3\cos^2\theta_n - 1\rangle_{\text{ODF}}|/4, \tag{2}$$

where S is given by the average of $(3\cos^2\theta_m - 1)/2$ over fluctuations of axis **m** around the director **n**, $\langle 3\cos^2\theta_a - 1\rangle_{\text{conf}}$ depends on the relative position of the resonant nuclei on the molecule and is weakly temperature dependent; usually it is incorporated in $\Delta\nu_0$ [20]. The factor $\langle 3\cos^2\theta_n - 1\rangle_{\text{ODF}}$ represents an average over the ODF modes whose relaxation rates are larger than $\Delta\nu$, which — in a typical nematic — decreases the line splitting by a few percents. The slow modes are not incorporated in the averaging process. Their contribution to $\Delta\nu$ depends on θ_n and results in an additional line broadening $\Delta\nu\langle\theta_n^2\rangle_{\text{slow ODF}}/2$, usually not larger than a few tens of Hz. Therefore, the NMR line splitting measurements offer a relatively convenient way of determining the nematic order parameter S but do not yield much information about molecular motion in the bulk.

Nuclear magnetic relaxation, which establishes the equilibrium distribution of the nuclear magnetization, is a dynamic process caused by time dependent dipolar or quadrupolar spin interactions. These fluctuations are directly related to the intensity and frequency distribution of the thermal motion of spin-bearing molecules. The relaxation rate is essentially a linear combination of the spectral densities $j_k(\omega)$ of the autocorrelation functions of the relevant interactions, expressed in frequency units as [11]

$$R = \sum_k A_k j_k(\omega), \tag{3}$$

where A_k are numerical factors of magnitude 1. The NMR frequency window depends on the method. Usually, one measures the spin-lattice relaxation time T_1 (i.e., R^{-1}), which characterizes the relaxation of the magnetization via exchange of the magnetic energy between the spin system and the lattice, and the spin-spin relaxation time T_2, which corresponds to the relaxation within the spin system itself. The spin-lattice relaxation rate T_1^{-1} contains the spectral densities at Larmor frequency ω_0 and at double Larmor frequency $2\omega_0$. In case of T_2^{-1}, there is an additional term at zero frequency that contributes to the relaxation as well. Sometimes the spin-lattice relaxation time is measured in the rotating frame resulting in the relaxation time $T_{1\rho}$. The corresponding relaxation rate depends on spectral densities at ω_0, $2\omega_0$ and ω_1 — the strength of the rotating magnetic field. A comprehensive spin relaxation study could thus indirectly provide valuable information about molecular dynamics covering the range from $10^3 - 10^{11}$ Hz [11–15].

If the dynamics of the system is characterized by a single correlation time τ, the spectral density is described by a single Lorenzian shape $j(\omega) \sim 2\Delta\omega_{\text{int}}^2\tau/[1+(\omega\tau)^2]$, where $\Delta\omega_{\text{int}}$ is the fluctuating part of the relevant interaction expressed in frequency units. It is useful to bear in mind the following situations:

- A motion with a short correlation time τ which fulfills the conditions $\omega_0\tau \ll 1$ produces practically equal relaxation times T_1, $T_{1\rho}$, and T_2, which are in this limit independent of frequency. Such a situation, when relaxation cannot provide much information, is often realized in simple isotropic liquids and nematic phases by conformational motion and individual molecular reorientation. Because of 180° flips, individual reorientations around the short molecular axes are not causing relaxation [11].
- A motion with τ^{-1} comparable to the Larmor frequency — usually between 10^8 to 10^9 Hz — ($\omega_0\tau \sim 1, \omega_1\tau \ll 1$) causes a significant difference between high frequency relaxation time T_1 and the low frequency ones T_2 and $T_{1\rho}$. This is the range covered by ODF's and the diffusion induced modulation of intermolecular interaction.
- Correlation times between 10^{-8} and 10^{-7} s, where $\omega_0\tau > 1$ and $\omega_1\tau < 1$ yield a ω_0^2-type frequency dependence of the relaxation time T_1 and frequency independent relaxation times T_2 and $T_{1\rho}$, which are also roughly equal in magnitude.
- Slow motion with $T_2 > \tau > 10^{-6}$ s, ($\omega_0\tau \gg 1$ and $\omega_1\tau \sim 1$) mostly affects T_2 and $T_{1\rho}$ and negligibly contributes to T_1. This is the range of very long wave length ODF's.

Usually the spectral density must be expressed as a sum of several Lorenzians. Suppose that the molecules undergo a fast but anisotropic motion with short correlation time which partially averages the nuclear dipolar or quadrupolar interaction. The remaining interaction may be modulated by another, slower motion. The two types of molecular motion can be treated as statistically independent and the total relaxation rate $R(T_1^{-1}, T_{1\rho}^{-1}$ or $T_2^{-1})$ simply consists of two contributions:

$$R = R_{\text{fast}} + R_{\text{slow.}} \tag{4}$$

In case of ODF's the sum must include spectral density contributions of all modes yielding the well known dispersion $(T_1^{-1})_{\text{ODF}} \propto \omega_0^{-1/2}$ valid in the upper kHz range [21, 22].

In addition to nuclear magnetic relaxation methods, the **pulsed gradient spin-echo (PGSE) technique** may also be used for studying the translational diffusion of molecules in a liquid crystal, its main advantage being a direct measurement of the diffusion coefficient [16]. In a pulsed gradient spin-echo experiment, the echo attenuation depends on parameters of the setup (magnetic field gradient, duration of gradient pulses, and diffusion time) and diffusion tensor.

3. MICROCONFINED SYSTEMS

Ordering and structures The ordering in confined systems is intrinsically inhomogeneous. The deformed structures are stabilized by the frustration induced by the shape and anchoring of confining surfaces. In systems where confinement occurs on a larger scale (usually 10 or more μm), the nematic ordering is well described by the director field and the so-called strong anchoring condition [17]. The director field can be determined by minimization of the Frank elastic free energy [17]. As an example, a schematic presentation of the director field in a spherical droplet with tangential anchoring is shown in Figure 2 (a, b). However, in microconfined systems the concept of strong anchoring is no more justified. If the temperature of the sample is not close to the nematic-isotropic phase transition and the size of the confining cavity is not much smaller than 1 μm, the orientational order parameter can be assumed to be spatially homogeneous and the director field is then simply obtained by minimization of elastic, surface and external field contributions to the free energy (see, for instance, Ref. [23]). In case of a more severe confinement, variations of the degree of order are no

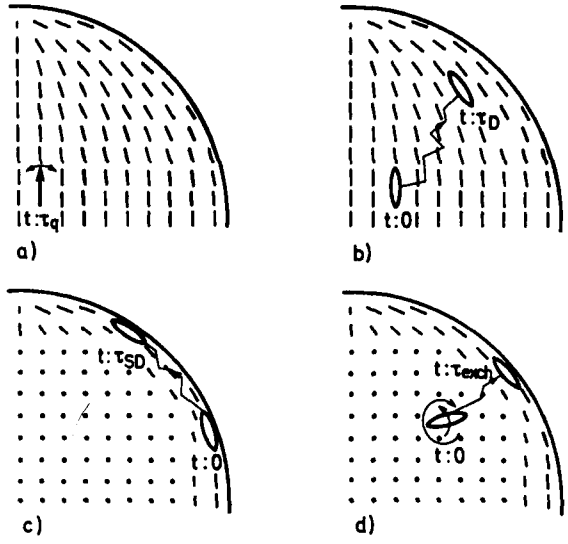

FIGURE 2 A qualitative representation of nematic (a and b) and paranematic ordering (c and d) in spherical cavities in case of tangential anchoring. The nematic structure (a, b) is bipolar, while the paranematic ordering is characterized by weakly ordered surface layers (c, d). The four types of molecular motion in confined liquid crystals are illustrated as well: order director fluctuations (a), translational diffusion (b), diffusion in the surface layer (c), and diffusion between ordered and disordered regions (d).

more localized to immediate vicinity of the boundary and the defects. The order parameter changes significantly over the correlation length introduced in Section 2. Usually the Landau-de Gennes formalism for nonuniform nematic phases [24] is used to determine the spatial dependence of the degree of the orientational order. The pretransitional ordering induced by confining surfaces, illustrated schematically in Figure 2 (c, d), can be treated in a similar way. This phenomenon was rather thoroughly studied in isotropic liquid crystal confined to cylindrical cavities [25] and constrained by dispersed polymer network [10].

Dynamics The drastic impact of the confinement on the ordering is reflected also in the dynamics of the liquid crystal. Let us here briefly examine the main effects.

In confined systems, the collective motion of liquid crystalline molecules—*order director fluctuations*—is modified due to surface coupling which affects the director dynamics in various aspects. First, it sets an upper limit for the wave lengths of the fluctuations, which is determined by the

characteristic size of the cavity; in bulk systems, the wave length of the fluctuation modes is not bound. The surface interaction also leads to additional dissipation of energy, usually described by the so-called surface rotational viscosity. And finally, the collective dynamics is intimately related to the confinement induced equilibrium structure: it may include defects, which modify the behavior of director fluctuations, and it may be transformed into another configuration, the transformation being mediated by unstable eigenmodes of director fluctuations [26].

The orientational ordering of confined systems varies rather slowly except at interfaces and close to defects. In enclosures with characteristic size much larger than correlation length, the effect of these regions is small. Therefore, the molecular self-diffusion among regions with different director orientations can be treated as a continuous process consistently described by the diffusion equation. The characteristic time scale of such *translation induced rotation* [illustrated in Fig. 2 (b)] is roughly given by $\tau_D = d^2/6D$, where d is a typical distance over which the orientational inhomogeneities become important (for a spherical droplet, this is its radius; for a polymer network, the interfiber distance, etc.). For $d \sim 100$ nm the modulation times are in the ms range.

Another rotational mechanism, similar to this one, is the *surface diffusion* [Fig. 2 (c)]. It occurs whenever the liquid crystalline molecules are strongly bonded to the surface but free to diffuse far enough along the curved boundary within the surface dwell time τ_s, which characterizes the average time spent by a liquid crystal molecule at the surface.

Molecular exchange in the surface layer, on the other hand, is a process in which the molecules experience a change in the degree of order when entering/leaving the surface layer [Fig. 2(d)] [20]. This effect is particularly important in case of significant surface-induced ordering. The characteristic time of this modulation is determined either by the surface dwell time τ_s or by the diffusion time $\xi^2/2D$ (during which the molecule leaves the interfacial layer), whichever is longer.

Fluctuating interfaces caused by the fluctuations of the confining matrix are expected to be relevant in systems with a low concentration of the polymer network dispersed in a liquid crystal background. In many aspects, they are similar to the order director fluctuations in nematic phases. Their dynamics is characterized by a wide distribution of correlation times. Excitation modes of wave vector $\mathbf{q}$ decay with the correlation time $\tau_q = \beta q^{-2}$, where β is a material-dependent constant [27].

4. LINE SHAPE AND MOTIONAL AVERAGING

In order to explain the NMR spectrum in the intermediate cases when motion is neither fast nor slow on the NMR time scale, the molecular motion is described within the time dependent Hamiltonian approximation. This approach leads to a general expression for the spectrum

$$I(\omega) = \int \exp(i\omega t) \left\langle \exp\left[i \int_0^t \omega(\mathbf{r}(t'))\, dt' \right] \right\rangle dt, \tag{5}$$

where $\omega(\mathbf{r}(t'))$ is the local value of the resonant frequency whose time dependence is governed by the molecular dynamics. The first study of the translation induced rotation in microconfined liquid crystals was concerned with nematic droplets. Here we are interested in the limiting cases where—depending on whether the dynamics is slow or fast compared to the observation frequency range—the spectrum either corresponds to static director field or consists of two lines reflecting diffusion induced motional averaging over the structure. The examples of spectra of α-deuterated 5CB and β-deuterated 8CB in cylindrical cavities with diameter 0.2 nm cover both limits (Fig. 3) [29, 30]. In the nematic phase of 8CB, homeotropic anchoring induced the radial escaped structure [6] and in the isotropic phase of 5CB a thin paranematic homeotropically oriented surface layer was observed. The nematic line splitting $\Delta\nu_{nem} \gg \tau_D^{-1}$ allows the use of the static distribution of the frequencies reflecting the director field (see spectra

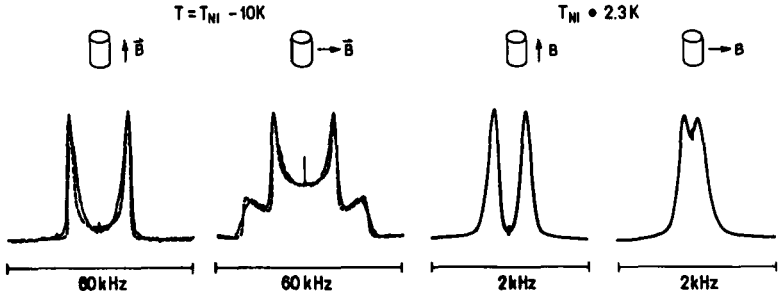

FIGURE 3 Experimental ^{2}H-NMR spectra of nematic 8CB-βd_2 in Nuclepore membranes (left) and isotropic phase of 5CB-βd_2 in Anopore membranes (right) for longitudinal and transverse orientation of magnetic field. The two nematic spectra nearly perfectly fit to the theoretical static spectrum (dashed lines) corresponding to the escaped radial structure with point defects [30]. The two isotropic spectra correspond to the complete motional averaging over the cylinder [29].

for two orientations of the magnetic field in Fig. 3). On the other hand, the paranematic splitting in the isotropic phase $\Delta\nu_{iso}$ is much smaller than the inverse diffusion time τ_D, indicating that a motional averaging caused by translational diffusion and molecular exchange in the surface layer can be expected. The observed lines for longitudinal and transverse orientation of cavities with respect to the magnetic field and, in particular, the reduction of the splitting to one half in the latter case (see the two spectra of the isotropic 5CB in Fig. 3) are completely consistent with these predictions.

5. NUCLEAR MAGNETIC RELAXATION IN MICROCONFINED SYSTEMS

In confined systems, the relaxation is generally nonuniform because of the inhomogeneous ordering and interfacial effects. The typical time for a molecule to reach the boundaries of a system, characterized by a distance d, is given by $\tau_D = d^2/6D$. Using the surface dwell time τ_s, one can specify the necessary conditions for the fast exchange limit, where a single relaxation rate R can be defined for each enclosure, as

$$\tau_D^{-1}, \tau_s^{-1}\eta \gg R_{free} \text{ and } \tau_s^{-1} \gg R_{surf}, \tag{6}$$

where η stands for the relative number of molecules in the surface layer and R_{free} and R_{surf} are the relaxation rates of freely diffusing molecules and molecules in the surface layer, respectively. The effective relaxation rate R is then given by a simple weighted sum

$$R = (1-\eta)R_{free} + \eta R_{surf}. \tag{7}$$

If the enclosures are of the same size or well interconnected (e.g., in polymer network systems), such a description is justified. We limit our further discussion to these cases bearing in mind that in general, the confining cavities can be well separated and nonuniform in size, shape, and orientation (as, for instance, in PDLC's). In such cases, distributions of relaxation rates $w(R)$—which can be used for an indirect determination of enclosure size, shape, or orientation distribution—are observed.

In the following we examine the relaxation rates related to the mechanisms relevant for the confined systems. It is worthwhile to point out that the relaxation rate of free molecules, R_{free}, is expected to be influenced by order director fluctuations and translation induced rotation, while the rate of

molecules in the surface layer, R_{surf}, is mostly affected by surface diffusion, surface fluctuations, and molecular exchange between ordered and disordered regions.

ODF's and structural transitions In confined liquid crystals, $(T_1^{-1})_{ODF}$ is independent of Larmor frequency for $\omega_0 < \omega_{0c}$, regardless whether the system is restricted in one, two, or three spatial dimensions [31]. The critical frequency is determined by the characteristic size (d) of the confining cavity: $\omega_{0c} \sim K/\gamma_1 d^2$, where K and γ_1 are the (average) elastic constant and the rotational viscosity of the liquid crystal, respectively. However, in vicinity of a structural transition—if it is allowed in a particular geometry—, the low-frequency spin-lattice relaxation rate should increase considerably due to critical slowing down of the order director fluctuations. Such a behavior can be perhaps most transparently studied in cylindrical microcavities where a temperature-driven transition from planar to escaped radial configuration is expected to take place just above the smectic-nematic phase transition [32].

A theoretical analysis of the temperature dependence of $(T_1^{-1})_{ODF}$ ($\omega_0 \to 0$) is based on a numerical procedure, introduced in Ref. [31]. Since the pretransitional behavior of the spin-lattice relaxation rate is dominated by the slowest eigenmodes, only these are taken into account.

The result, based on experimental data for temperature dependence of the elastic constants and the rotational viscosity of 8CB [33, 34], is shown in Figure 4. For the above parameters the critical frequency ω_{0c} is approximately equal to 30 kHz. As indicated in Figure 4, the structural transition from planar to escaped radial configuration should take place at 3.5° C above the Sm-N phase transition. As predicted, the low-frequency limit of the spin-lattice relaxation rate diverges on approaching the structural transition. In this particular case the capillaries are assumed to be perpendicular to the direction of the magnetic field, but the effect would be qualitatively the same for any orientation of the sample. Obviously, such an experiment—though not easily performable—could yield valuable information on stuctural transitions in confined liquid crystals and their mechanisms.

Translation induced rotation In the section on line shape and motional averaging we have stressed that in the regime of complete motional averaging over the whole liquid crystal structure ($\Delta\nu \ll \tau_D^{-1}$) the spectrum cannot yield any information on the time scale of the motion. In microconfined systems, the alignment of the liquid crystal often prevents also the use of pulsed gradient spin-echo techniques. Therefore, indirect magnetic relax-

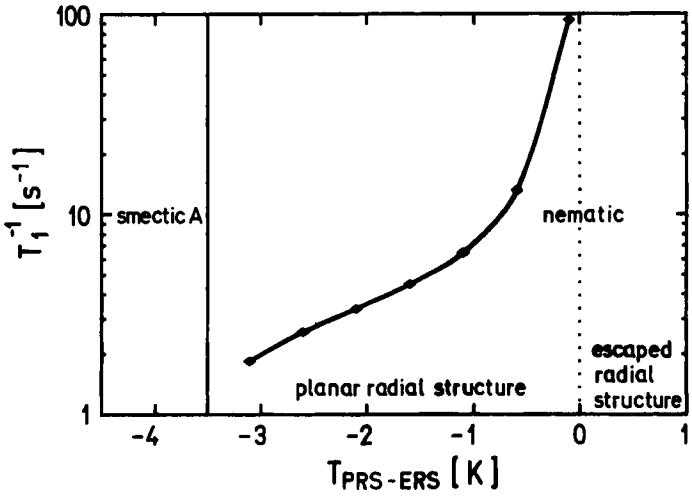

FIGURE 4 A temperature-driven structural transition in cylindrical capillaries with $R = 100$ nm, filled with 8CB, as it should be seen by the low-frequency spin-lattice relaxation rate measurement. The transition from planar to escaped radial structure should take place at approximately 3.5 K above the smectic-nematic phase transition. The calculated values of $T_1^{-1}(\omega_0 \to 0)$ are plotted with dots; the solid line serves just as a guide to the eye.

ation approach is the only NMR method which can offer an insight into the diffusion dynamics in these systems. The relaxation caused by translation induced rotation has been discussed in detail for nematic droplets in PDLC materials [35]. The frequency dependence of $T_{1\rho}$ in such a medium, presented in Figure 5, clearly demonstrates the importance of the diffusion induced reorientation in low ω_1 frequency regime. The calculation of the spectral densities is based on the bipolar structure [Fig. 2 (a,b)] obtained by the minimization of the Frank elastic free energy. It should be emphasized that in this case the droplet diameter $\sim 1\mu$m does not allow us to assume that averaging of the relaxation rate takes place: one has to examine the distribution of $w(T_{1\rho}^{-1})$. The fit of the experimental data was performed using the dominant relaxation rate [35].

Molecular exchange in the surface layer Here we focus our attention to the case where exchange between partially ordered surface layer and disordered isotropic material at distances $\gg \xi$ from the boundary occurs [Fig. 2 (d)]. This exchange is controlled by temporary bonding of the molecules on the surface (surface dwell time τ_s) and by diffusion from the ordered to the disordered areas and vice versa (diffusion time $\xi^2/2D$.). The effective dipolar or quadrupolar nuclear interaction, averaged over all faster molecular

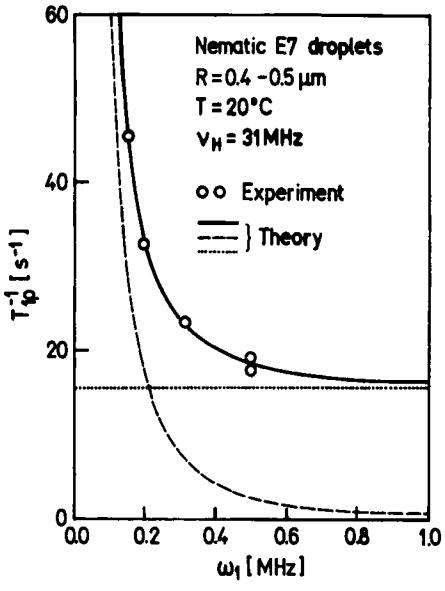

FIGURE 5 A comparison of theoretical and experimental $T_{1\rho}^{-1}(\omega_1)$ data for droplets of nematic liquid crystal E7 [35]. The solid line represents the sum of contributions of translation induced reorientation (dashed line) and other relaxation mechanisms (dash-dotted line).

reorientations, is modulated on a slower time scale characterized by the exchange time of molecules τ_{exch}. As we will see later, the experimental evidence indicates that $\tau_{exch} \approx \tau_s$.

The exchange significantly affects only T_2 and $T_{1\rho}$ of the surface fraction of the molecules. According to Eq. (7), the contributions of molecular exchange between the ordered and disordered regions to the two deuteron relaxation rates are

$$(T_{1\rho}^{-1})_{exch} = \eta \Delta\omega_{Q\rho}^2 \frac{2\tau_s}{1+(2\omega_1\tau_s)^2}, \tag{8}$$

$$(T_2^{-1})_{exch} = 2\eta \Delta\omega_{Q2}^2 \tau_s. \tag{9}$$

$\Delta\omega_{Q\rho}$ and $\Delta\omega_{Q2}$ are of the same magnitude and measure the strength of the deuteron quadrupolar coupling averaged over all fast types of motion. Therefore, both of them are proportional to $S_0^2\langle(3\cos^2\theta_n - 1)^2\rangle/4$, where S_0 is the value of the order parameter at the surface and the brackets denote the spatial average.

Since the ordered surface layer persists far above the transition temperature, the effectiveness of the exchange mechanism extends over a wide range of the isotropic phase. The exchange-induced relaxation rate was observed in studies of PDLC materials [36, 37], filled porous Anopore membranes [38] (Fig. 6), and liquid crystals constrained by low-concentration polymer network [20]. In Figure 7 the results of the latter study are summarized. The increase of the spin-spin and spin-lattice relaxation rates in the rotating frame with respect to its counterparts in corresponding bulk systems can be understood in terms of Eqs. (8) and (9). Using the ω_1-frequency dependence of $T_{1\rho}^{-1}$ and T_2^{-1} data of 5CB constrained by polymer network, both surface dwell time $\tau_s \sim 4$ μs and surface order parameter $S_0 \sim 0.1$ are determined. In case of Anopore membranes permeated with liquid crystal, the T_2 data alone are somewhat less informative [38]. Nevertheless, together with the NMR line splitting data [25] (which provide values for S_0) the dwell time τ_s was estimated to be 40 μs in case of chemically treated cavity walls inducing homeotropic anchoring and 10 μs in case of untreated membranes.

Surface diffusion The two dimensional diffusion of molecules along the surface modulates the nuclear spin coupling via translation induced rotation whenever the surface is not perfectly planar [Fig. 2 (c)]. It has been shown that the relaxation induced by this type of motion reflects not only the shape of the cavity but also the characteristics of the surface roughness [39].

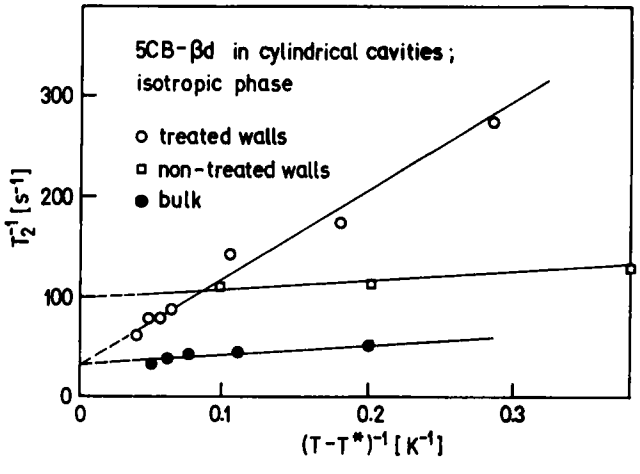

FIGURE 6 Deuteron spin-spin relaxation rate as a function of $(T-T^*)^{-1}$ in isotropic 5CB, confined in treated and untreated Anopore membranes [38]; T_2^{-1} in bulk sample (solid circles) is also plotted for comparison. The surface dwell time, τ_s, can be determined from the slope of the fitted lines.

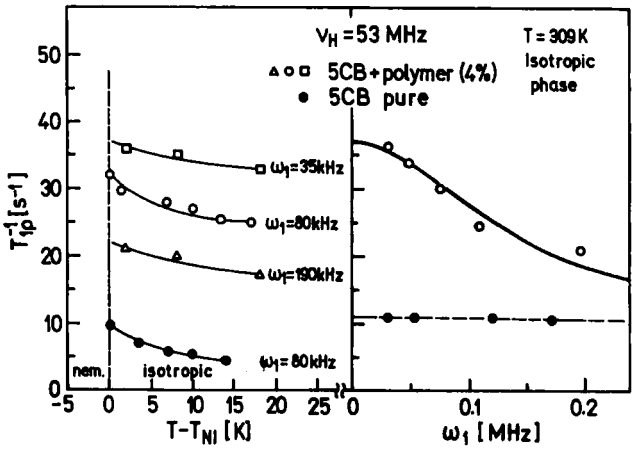

FIGURE 7 Temperature dependence of $T_{1\rho}^{-1}$, the proton spin-lattice relaxation rate in the rotating frame, in the isotropic 5CB with 4% polymer network and in bulk isotropic sample for various frequencies ω_1; ω_1 frequency dependence of $T_{1\rho}^{-1}$ for the two systems at $T - T_{NI} = 2$ K [20].

The correlation function for this type of molecular motion can be expressed as sum over Fourier components with wave vectors (**q**) corresponding to modulation of the confining surface, the terms of the sum being given by $G_q(t) = \exp(-t/\tau_q)$ with

$$\tau_q = \frac{1}{D_\parallel q^2}, \tag{10}$$

where $D_\parallel$ is the lateral translational diffusion coefficient. This mechanism is effective for relaxation of both protons and deuterons in the nematic as well as in the isotropic phase. In the latter case, however, its effect might be masked by the exchange induced relaxation.

Surface fluctuations Network fluctuations, introduced in Section 3, influence the relaxation of protons and deuterons on liquid crystal molecules bound on the network surface. However, a liquid crystal molecule, which is on the average bound to the surface for a time τ_s, experiences only the orientational fluctuations of the fibers with correlation times τ_q shorter than τ_s. The modulation of residual dipolar or quadrupolar interaction by network fluctuations is thus much weaker than in the exchange process where the coupling varies between zero and its value at the surface.

Since in this case $\tau_q < \tau_s$ as well as $\tau_q < \tau_D$, it is reasonable to assume that $(T_1^{-1})_{\text{fluct}}$ is generally overwhelmed by $(T_1^{-1})_{\text{exch}}$, which is larger. Nevertheless, the importance of network fluctuations cannot be ruled out without performing frequency dispersion measurements over several decades. It should be noted that the fluctuations of the network influence indirectly $(T_2^{-1})_{\text{exch}}$ by diminishing the residual interaction.

Cross relaxation It should be mentioned that in the case of proton magnetic resonance in liquid crystals confined in cavities with organic boundaries, the cross relaxation (i.e. direct transfer of nuclear magnetization between the liquid crystal and confining matrix protons) may enhance the relaxation rates [40]. The transfer is caused by mutual spin flips of bound liquid crystal protons and polymer protons. The time, characteristic for the transfer of magnetization, τ_{cross}, depends on the strength of the dipolar interaction between the two types of spins and on the average dwell time of liquid crystal molecules in the surface layer τ_s. In PDLC materials the cross-relaxation was found to dominate the proton relaxation in a broad frequency range. The cross-relaxation rate was also measured directly [41, 42] and related to the strength of dipolar interaction between interfacial spins.

6. NMR DETECTION OF RESTRICTED MOLECULAR DIFFUSION

The translational molecular motion in bulk liquid crystalline materials is characterized by the anisotropy of the diffusion tensor. In confined systems, the diffusion of the molecules is no longer unbound because of the restricted geometry itself. In addition, the geometry-induced inhomogeneous liquid crystalline structure may alter the diffusion tensor and the molecular motion can be modified by the interaction of the molecules with the walls of the confining cavity. In many cases, however, the restricted geometry becomes the predominant feature of the molecular diffusion in restricted liquid crystalline systems, particularly when the size of the confining cavity is rather small.

This assumption is the usual starting point for the interpretation of the pulsed gradient spin-echo measurements in confined systems. The theoretical parts of such analyses are focused on the calculation of the spin-echo attenuation. The attenuation functions for planar, cylindrical, and spherical geometry were already derived within the approximation of infinitely narrow gradient pulses [43, 44]. However, in microconfined liquid

crystalline systems with characteristic size $\sim$ 100 nm (e.g. cylindrical cavities of Anopore and Nuclepore membranes, spherical cavities in PDLCs) this approximation usually cannot be used because τ_D is comparable to the duration of gradient pulses, which are typically in the ms range.

In this case, the attenuation can be calculated by integration of the Bloch-Torrey equation which describes the evolution of the nuclear magnetization. The molecular motion within an infinite cylinder can be factorized into unrestricted diffusion along the cylinder and restricted planar motion, perpendicular to the axis. This means that the attenuation may also be decomposed in the same manner

$$A(\mathbf{g},\delta,\Delta) = A_{\parallel}(g_{\parallel},\delta,\Delta)\cdot A_{\perp}(g_{\perp},\delta,\Delta) \tag{11}$$

where $g_{\parallel}$ and $g_{\perp}$ are longitudinal and transverse component of the magnetic field gradient $\mathbf{g}$, respectively; δ is the duration of the gradient pulse and Δ is the diffusion time. It can easily be shown that $A_{\parallel} = \exp[-((\gamma\delta_{g\parallel})^2 D\Delta)]$ [43], where γ is the gyromagnetic ratio.

In cylindrical coordinates and with the spin-spin relaxation factored out,

$$\frac{\partial M}{\partial t} = -i\,[\alpha(t) r\cos\varphi]\,M + \nabla^2 M, \tag{12}$$

where $M = M_x + iM_y$ is the in-plane magnetization in complex notation and

$$\alpha(t) = \begin{cases} R^3\gamma g_{\perp}/D & \text{during the pulses} \\ 0 & \text{otherwise} \end{cases} \tag{13}$$

is the magnitude of the dimensionless magnetic field gradient, applied along the x-axis. In Eq. (12), dimensionless time and spatial coordinates are used: $r \leftarrow \sqrt{x^2+y^2}/R$ and $t \leftarrow t/(R^2/D)$, where R is the radius of the capillary. In the following, pulse width δ and diffusion time Δ are expressed in units of R^2/D as well. —Since the diffusion current normal to the wall of the capillary must be zero, the boundary condition at $r = 1$ is $\partial M/\partial r = 0$ and the initial condition after preparation of the magnetization of the sample is $M(\mathbf{r}, 0) = 1$.

In order to compute the attenuation of the spin echo, Eq. (12) is integrated numerically from $t = 0$ to $t = 2\Delta$. At $t = \Delta$ the transformation $M(\mathbf{r},\Delta+) = M\ (\mathbf{r},\Delta-)^*$ is performed to take into account the effect of the

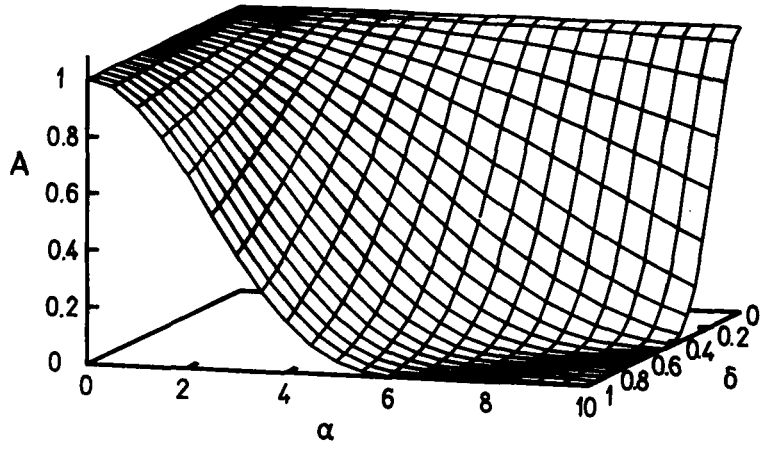

FIGURE 8 The dependence of the spin-echo attenuation $A_\perp$ on magnetic field gradient (α) and pulse width (δ) in the limit of infinite diffusion time ($\Delta \to \infty$). For large gradient strengths and pulse widths, the attenuation is a non-monotonous function of α and δ. This behavior is qualitatively the same as in other restricted geometries [44].

spin reversal. The attenuation is given by the average of the x-component of the magnetization at $t = 2\Delta$

$$A_\perp(\alpha, \delta, \Delta) = \frac{1}{2\pi} \int [M(\mathbf{r}, 2\Delta) + M^*(\mathbf{r}, 2\Delta)] dV. \tag{14}$$

In Figure 8, the dependence of $A_\perp(\alpha, \delta, \Delta \to \infty)$ on α and δ is shown. The attenuation function is in principle non-monotonous; however, the magnitude of the spin-echo in this nonmonotonous regime is rather small and thus not easily observable.

These results can be used in the interpretation of the measurements of the diffusion coefficients in liquid crystals (and liquids in general), confined in cylindrical capillaries. On the other hand, they can also be used to image the microstructure of the embedding material. Since the method is sensitive only to translational motion of the molecules, the data analysis is in principle relatively straightforward, though the situation is somewhat less transparent if surface relaxation mechanisms or similar phenomena are present.

7. CONCLUSIONS

The basic methods of nuclear magnetic relaxation and resonance offer a rather complete and detailed insight into the dynamics of liquid crystals,

covering a broad range of time scales from 10^{-3} to 10^{-11} s. They are particularly sensitive to phenomena specific to severely restricted systems (e.g. two dimensional diffusion along the confining surface, exchange of molecules between surface-aligned layer and disordered interior, etc.).

Most of the confinement related phenomena occur on relatively long time scale, reducing the range of suitable methods to low frequency T_1, $T_{1\rho}$, and T_2 studies. Line shape analyses are complementary to the relaxation time measurements and offer information on types of motion which are too slow to be studied by the latter. In case of fast motion, the line shape provides only information on its anisotropy and amplitude. The spin-echo studies of diffusion are relevant mostly for well aligned nematic structures and for the isotropic phase.

In the review, we do not discuss more complex NMR methods such as two dimensional NMR (see Ref. [36] and references therein). Finally, it should be stressed that the NMR techniques are integrative in nature and — unlike, for instance, light scattering and other optic methods — cannot provide a selective insight into the dynamics of liquid crystalline systems.

Support from Ministry of Science and Technology of Slovenia (grant No. 11-7470-0106-96) and European Union (grant No. CIPA-CT93-0159) is Acknowledged.

References

[1] J. W. Doane, N. A. Vaz, B. G. Wu and S. Žumer, *Appl. Phys. Lett.*, **48**, 269 (1986).
[2] P. P. Crooker and D. K. Yang, *Appl. Phys. Lett.*, **57**, 2529 (1990).
[3] J. Pirš, R. Blinc, B. Marin, I. Muševič, S. Pirš and J. W. Doane, *Mol. Cryst. Liq. Cryst.*, **258**, 621 (1995).
[4] J. W. Doane, in *Liquid Crystals: Applications and Uses*, edited by B. Bahadhur, (World Scientific, Singapore, 1990), Chap. 14, and references therein.
[5] G. P. Crawford and S. Žumer, (eds.) *Liquid Crystals in Complex Geometries* (Taylor and Francis, London, 1996); P. Drzaic, *Liquid Crystal Dispersions* (World Scientific, Singapore, 1995).
[6] G. P. Crawford, M. Vilfan, J. W. Doane, and I. Vilfan, *Phys. Rev., A* **43**,835 (1991).
[7] G. P. Crawford, D. W. Allender, J. W. Doane, M. Vilfan and I. Vilfan, *Phys. Rev., A* **44**, 2570 (1991).
[8] G. S. Iannacchione, G. P. Crawford, S. Žumer, J. W. Doane and D. Finotello, *Phys. Rev. Lett.*, **71**, 2595 (1993).
[9] T. Bellini, N. A. Clark, C. D. Muzny, L. Wu, C. W. Garland, D. W. Schaefer and B. J. Oliver, *Phys. Rev. Lett.*, **69**, 788 (1992).
[10] G. P. Crawford, A. Scharkowski, Y. K. Fung, J. W. Doane and S. Žumer, *Phys. Rev., E* **52**, R1273–R127 (1995).
[11] A. Abragam, *Principles of Nuclear Magnetism* (Oxford University Press, Oxford, 1967).
[12] J. W. Doane, *NMR of Liquid Crystals*, in *Magnetic Resonance of Phase Transitions*, edited by F. J. Ownes, *et al.* (Academic Press, New York, 1979).
[13] F. Noack, *Prog. NMR Spectr.*, **18**, 171 (1986).

[14] K. Kohlhammer, K. Müller and G. Kothe, *Liq. Cryst.*, **5**, 1525 (1989).
[15] F. Grinberg and R. Kimmich, *J. Chem. Phys.*, **103**, 365 (1995).
[16] P. T. Callaghan, *Principles of Nuclear Magnetic Resonance Microscopy* (Clarendon Press, Oxford, 1993).
[17] P. G. de Gennes and J. Prost, *The Physics of Liquid Crystals* (Clarendon Press, Oxford, 1993).
[18] G. Krüger, *Phys. Reports.*, **82**, 229 (1982).
[19] P. Palffy-Muhoray, E. C. Gartland and J. R. Kelly, *Liq. Cryst.*, **16**, 713 (1994).
[20] M. Vilfan, G. Lahajnar, I. Zupančič, S. Žumer, R. Blinc, G. P. Crawford and J. W. Doane, *J. Chem. Phys.*, **103**, 8726 (1995).
[21] P. Pincus, *Solid State Commun.*, **7**, 415 (1968).
[22] W. Wölfel, F. Noack and S. Stohrer, *Z. Naturforsch, Teil A* **30**, 437 (1978).
[23] S. Kralj and S. Žumer, *Phys. Rev., E* **51**, 366 (1995).
[24] S. Kralj, S. Žumer and D. W. Allender, *Phys. Rev., A* **43**, 2943 (1991).
[25] G. P. Crawford, R. J. Ondris-Crawford, S. Žumer and J. W. Doane, *Phys. Rev. Lett.*, **70**, 1838 (1993).
[26] P. Palffy-Muhoray, A. Strigazzi, and A. Sparavigna, *Liq. Cryst.*, **14**, 1143 (1993).
[27] P. G. de Gennes, *Scaling Concepts in Polymer Physics* (Cornell University Press, New York, 1979).
[28] A. Golemme, S. Žumer, J. W. Doane and M. E. Neubert, *Phys. Rev., A* **37**, 559 (1988).
[29] G. P. Crawford, R. Stannarius and J. W. Doane, *Phys. Rev., A* **44**, 2558 (1991).
[30] R. J. Ondris-Crawford, G. P. Crawford, J. W. Doane, S. Žumer, M. Vilfan and I. Vilfan, *Phys. Rev., E* **48**, 1998 (1993).
[31] P. Ziherl, M. Vilfan, and S. Žumer, *Phys. Rev., E* **52**, 690 (1995).
[32] P. E. Cladis and M. Kléman, *J. Phys.* (France) **33**, 591 (1972).
[33] H. Hakemi, *Liq. Cryst.*, **5**, 327 (1993).
[34] P. Chattopadyay and S. K. Roy, *Mol. Cryst. Liq. Cryst.*, **237**, 1 (1993).
[35] S. Žumer, S. Kralj and M. Vilfan, *J. Chem. Phys.*, **91**, 6411 (1989).
[36] J. Dolinšek, O. Jarh, M. Vilfan, S. Žumer, R. Blinc, J. W. Doane and G. P. Crawford, *J. Chem. Phys.*, **95**, 2154 (1991).
[37] D. Schwarze, F. Noack, M. Vilfan and G. P. Crawford, to be published.
[38] N. Vrbančič, M. Vilfan, R. Blinc, J. Dolinšek, G. P. Crawford and J. W. Doane, *J. Chem. Phys.*, **98**, 3540 (1993).
[39] G. Schauer, R. Kimmich and W. Nusser, *Biophys. J.*, **53**, 397 (1988).
[40] H. T. Edzes and E. T. Samulski, *J. Magn. Reson.*, **31**, 207 (1978).
[41] O. Jarh, A. Sepe and M. Vilfan, Abstracts of 10th Experimental NMR Conference, Veldhoven (1991).
[42] C. W. Cross and B. M. Fung, *J. Chem. Phys.*, **96**, 1425 (1992).
[43] J. E. Tanner and E. O. Stejskal, *J. Chem. Phys.*, **49**, 1768 (1968).
[44] P. T. Callaghan, *J. Magn. Reson., A* **113**, 53 (1995).